Research Article

Changes in Extracellular Matrix Gene and Protein Expressions in Human Trabecular Meshwork Cells in Response to Mechanical Fluid Flow Stimulation

Short title: Mechanical Fluid Flow Stimulation of HTM Cells

Koichi Yoshida[1,2†], Motofumi Kawai[1†*], Tsugiaki Utsunomiya[1‡], Akihiro Ishibazawa[1‡], Young-Seok Song[1], Mariana Sayuri B. Udo[1], Yoshikazu Tasaki[2], Akitoshi Yoshida[1]

1 Department of Ophthalmology, Asahikawa Medical University, Asahikawa, Hokkaido, Japan, **2** Department of Hospital Pharmacy & Pharmacology, Asahikawa Medical University, Asahikawa, Hokkaido, Japan

***** m-kawai@poem.ocn.ne.jp

[†]These authors contributed equally to this work.

[‡]These authors also contributed equally to this work.

Abstract

Purpose

To investigate the changes in extracellular matrix (ECM) gene and protein expressions in human trabecular meshwork (HTM) cells in response to mechanical fluid flow stimulation.

Methods

HTM cells were cultured on a glass plate and exposed to shear stress (0, 0.2, and 1.0 dyne/cm^2) for 12 hours. Changes in gene expressions were evaluated using microarray analysis. The representative genes related to ECM metabolism underwent real-time reverse-transcriptase polymerase chain reaction. Fibronectin (FN) and collagen (COL) IV levels in the supernatant were evaluated using immunoassays. Rho-associated coiled-coil-containing protein kinase (ROCK) activity also was investigated.

Results

After stimulation, transforming growth factor β2 mRNA levels were significantly ($p < 0.01$) lower than that of the static control (0 dyne/cm^2 for 12 hours). Matrix metalloproteinase 2 mRNA levels were significantly ($p < 0.05$) higher than the static control. COL type 1 alpha 2 mRNA, COL type 4 alpha 2 mRNA, and COL type 6 alpha 1 mRNA levels were significantly ($p < 0.05$, < 0.01, and < 0.05, respectively) higher than

the static control. The mean ± standard deviation FN levels (ng/mL) in the supernatant after stimulation (0, 0.2, 1.0 dyne/cm^2) were 193.7 ± 7.6, 51.5 ± 21.8, and 34.9 ± 23.6, respectively ($p < 0.01$). The FN and COL IV levels and ROCK activity were significantly ($p < 0.01$ and < 0.05, respectively) lower than the static control.

Conclusions

Changes in gene and protein expressions related to ECM metabolism occurred in HTM cells after stimulation. Specifically, the suppression of FN and COL IV production might explain the importance of mechanical fluid flow stimulation on maintenance of the normal aqueous humor outflow.

Keywords: trabecular meshwork, shear stress, aqueous humor, extracellular matrix, glaucoma, intraocular pressure

Introduction

Intraocular pressure (IOP) is maintained through a proper function of the aqueous humor, which is produced by the ciliary body [1]. About 70% to 95% of the aqueous humor drains through the conventional outflow pathway [2].Therefore, normal function of this outflow component is important to the IOP homeostasis and prevention of glaucoma [3]. Increased aqueous outflow resistance in this component is the main cause of glaucoma accompanied by elevated IOP [4, 5].

The trabecular meshwork (TM), juxtacanalicular meshwork, and Schlemm's canal, the collector channels, and the episcleral veins comprise conventional outflow pathway. Among those, extracellular matrix (ECM) in TM tissue, which are composed of collagen (COL) or fibronectin (FN) [6], is critical for the homeostatic maintenance of the normal outflow resistance [7]. Of note, recent studies revealed that ECM turnover is regulated by mechanical stress, at least in part [8-10].

Experimentally, mechanical stretching to TM cells upregulates gelatinase A and membrane type-1 matrix metalloproteinase (MMP) and reciprocally downregulates tissue inhibitors of metalloproteinases (TIMP)-2 [11]. Additionally, mechanical stretching by pulsatile IOP decreases outflow facility of both human and porcine anterior segments [12]. Moreover, cyclic mechanical stress alters the contractility of the TM cells [13].

Mechanistically, the mechanosensitive receptors on the TM cell surface reportedly sense the deformation of the ECM resulting from the IOP fluctuations via integrin-based cell-matrix contact [14, 15]. Collectively, these findings suggest that mechanical stress applied to the TM cells is important for the ECM turnover.

Clinically, it is generally considered that the TM function (e.g., ECM synthesis, phagocytosis, contractility) deteriorates after glaucoma filtration surgery or development of peripheral anterior synechia over a long period. In addition, the aqueous outflow to the TM after filtration surgery decreases to about 10% of the preoperative level [16], because most of the aqueous humor drains thorough trabeculectomy hole to the filtering bleb, fueling speculation that the mechanical fluid flow stimulation by aqueous outflow to the TM also has an important role in maintaining the TM function. However, to our knowledge, no previous reports have focused on the effect of mechanical fluid flow stimulation on TM cells and its effect on ECM turnover, although the effects of mechanical stimulation by stretching on TM cells have been previously investigated [8-11].

In the current study, to elucidate the role of mechanical fluid flow stimulation on the ECM metabolism in the TM, we applied mechanical fluid flow stimulation to the human trabecular meshwork (HTM) cells and investigated the gene and protein changes related to

93 the ECM metabolism. In addition, because Rho-associated coiled-coil-containing protein
94 kinase (ROCK) is related to the regulation of ECM component expression [17], the ROCK
95 activity also was investigated.
96

97 Materials and methods

98 Cell culture

99 The primary HTM cells obtained from ScienCell (Cat. No. 6590, Lot No. 3423, Carlsbad,
100 CA, USA) were maintained in Fibroblast Medium (ScienCell) containing 5% fetal bovine
101 serum and fibroblast growth supplements and penicillin/streptomycin (FGS, P/S solution,
102 ScienCell), according to the manufacturer's protocol. The HTM cells were cultured at the
103 bottom of poly-L-lysine-coated flasks (2 μg/cm^2). The cultured cells were passaged with
104 0.05% trypsin 2 mM ethylenediaminetetraacetic acid solution and seeded on glass plates
105 (70 × 100 × 1.3 mm) (Matsunami Glass, Kishiwada, Japan) coated with 0.02% type I
106 collagen (Angio-Proteomie, Boston, MA, USA). We used the HTM cells from between
107 passages 5 and 7. The current study was performed in accordance with the tenets of the
108 Declaration of Helsinki.

109 Shear stress experiments

110 Shear stress was applied to the confluent HTM cells using a parallel plate-type flow

chamber. We previously described the shear stress experiments [18-20]. Briefly, this flow circuit included a flow chamber, a peristaltic pump (SJ1220, ATTO, Tokyo, Japan), and a medium reservoir connected using silicone tubes. The culture medium was circulated continually with a peristaltic pump in an incubator at 37°C with 5% carbon dioxide. The shear stress inside the flow chamber was calculated by the formula, $\tau = \mu \cdot 6Q/a^2b$, where τ is the shear stress (dyne/cm^2), μ is the viscosity of the perfused fluid (0.00796 poise), Q the volumetric flow rate (mL/s), a the flow channel height (0.04 cm), and b the flow channel width (5.5 cm) in the cross section. To generate shear stress using a perfused medium, we used Dulbecco's Modified Eagle's medium (Wako Pure Chemical Industries, Ltd., Osaka, Japan) supplemented with 100 U/mL penicillin and 100 μg/mL streptomycin sulfate and GlutaMAX-I supplement (Life Technologies, Carlsbad, CA, USA) without serum. The medium viscosities were measured using a viscometer (ViscoLab 4000, Japan Controls, Tokyo, Japan). In the current study, the HTM cells were exposed to the following magnitudes of laminar shear stress: 0 dyne/cm^2 (static control) and 0.2 and 1.0 dyne/cm^2. After exposure to fluid flow for 12 hours, the glass plates on which the HTM cells were cultured were removed from the flow chamber and rinsed in phosphate buffered saline (PBS), and the HTM cells were collected

Microarray analysis for gene expressions

A DNA microarray assay was performed by Hokkaido System Science (Sapporo, Japan). Briefly, the total RNA from the HTM cells was amplified and transcribed into fluorescent cRNA using a Low Input Quick Amp Labeling Kit, One Color (Agilent Technologies, Santa Clara, CA, USA). The labeled cRNA was purified using an RNeasy Mini Spin Kit (QIAGEN, Germantown, MD, USA) and hybridized to the human microarray kit (SurePrint G3 Human GE 8 × 60 K version 3.0, Agilent Technologies). The raw data were normalized using a Gene Spring Software (version 13.0, Agilent Technologies). The normalized microarray data then were compared with the real-time RT-PCR analysis.

Real-time RT-PCR analysis for representative genes related to ECM metabolism

The HTM cells were collected with a scraper, and the total RNA was extracted using a NucleoSpin RNA kit (Takara, Shiga, Japan). The total RNA (25 μg/mL) underwent reverse transcription using a Transcriptor First Strand cDNA Synthesis Kit (Roche, Basel, Switzerland), according to the manufacturer's instructions, after which real-time PCR was performed using the Universal ProbeLibrary and Light Cycler 480 (Roche). The specific primer pairs are shown in Table 1. For all amplifications, the cycling conditions were as follows: an initial denaturation period for 5 minutes at 95°C, followed by 45 cycles of 10 seconds at 95°C, 30 seconds at 60°C, and 1 second at 72°C. The quantification of each gene expression signal was normalized with respect to the signal for the *glucose-6-*

147 *phosphate dehydrogenase* (*G6PDH*) gene. The relative fold changes in the expression of

148 each gene were determined using the $2^{-\Delta\Delta Ct}$ method.

149 **Table 1**. **Primer Sequences Used for Gene Expression Analysis by Real-Time RT-**

150 **PCR**.

Gene	Accession Number	Forward Primer	Reverse Primer
TGF-β2	NM_003238	CCAAAGGGTACAATGCCAAC	CAGATGCTTCTGGATTTATGGTATT
COL1A2	NM_000089	GGTCTCGGTGGGAACTTTG	CCAGGTGGGCCTCTAGGT
COL4A2	NM_001846	CAAAAGGAAGAGCAGGCTTC	CGTCGCCTTCTGTACATCTG
COL6A1	NM_001848	GAAGAGAAGGCCCCGTTG	CGGTAGCCTTTAGGTCCGATA
FN1	NM_212482	GACGCATCACTTGCACTTCT	GCAGGTTTCCTCGATTATCCT
MMP2	NM_004530	CCCCAAAACGGACAAAGAG	CTTCAGCACAAACAGGTTGC
TIMP2	NM_003255	GAAGAGCCTGAACCACAGGT	CGGGGAGGAGATGTAGCAC
G6PDH	NM_000402	CTGCAGATGCTGTGTCTGGT	TGCATTTCAACACCTTGACC

151 TGF-β2, transforming growth factor β2; COL1A2, collagen type 1 alpha 2; COL4A2,

152 collagen type 4 alpha 2; COL6A1, collagen type 6 alpha 1; FN1, fibronectin 1.

153 **Enzyme-linked immunosorbent assay (ELISA) for detecting FN levels**

154 FN in the culture medium supernatant was measured using an ELISA kit (R&D Systems,

155 Minneapolis, MN, USA), according to the manufacturer's instructions. Culture medium

156 supernatants were collected from the HTM cells with or without exposure to shear stress

157 for 12 hours. The optical density of the samples and fibronectin standard were determined

158 using a microplate reader.

Western blot analysis for detection of FN and COL IV levels

The HTM cells were washed with PBS and lysed with RIPA Lysis Buffer (Merck Millipore, Darmstadt, Germany) containing protease inhibitor cocktail tablets (Roche) and phosphatase inhibitor cocktail tablets (Roche) and phenylmethylsulfonyl fluoride. The lysates then were centrifuged at 13,000 rpm for 20 min at 4°C, and the resultant supernatants were collected. The total protein concentration was measured using a NanoDrop Fluorospectrometer (Thermo Fisher Scientific, Waltham, MA, USA). Equal amounts of protein were loaded into each well and separated by sodium dodecyl sulfate polyacrylamide gel electrophoresis and subsequently transferred to nitrocellulose membranes by electroblotting. The membranes were blocked with PVDF Blocking Reagent (Toyobo, Osaka, Japan) and incubated in Can Get Signal (Toyobo) containing the following antibodies for 1 hour: monoclonal β-actin antibodies (mouse, #3700, 1:2000 dilution) (Cell Signaling Technology, Danvers, MA, USA), polyclonal FN antibodies (rabbit, F3648, 1:1000 dilution), (Sigma-Aldrich, St. Louis, MO, USA), polyclonal COL IV antibodies (rabbit, SAB4500369, 1:1000 dilution) (Sigma-Aldrich), and horseradish peroxidase-conjugated anti-rabbit or anti-mouse IgG secondary antibody (#7076 and #7074, 1:10000 dilution) (Cell Signaling Technology). The membranes were exposed to ECL Prime Western Blotting Detection Reagent (GE Healthcare, Piscataway, NJ, USA)

and examined using LAS-3000 Imager (Fujifilm, Tokyo, Japan).

ROCK activity analysis

The cell lysates were collected from the HTM cells with or without exposure to shear stress for 12 hours. The total protein concentration was measured using a NanoDrop Fluorospectrometer. Equal amounts of protein then were measured by an ELISA using a 96-well ROCK Activity Assay Kit (Cell Biolabs, San Diego, CA), according to the manufacturer's instructions. Absorbance were measured on a microplate reader at 450 nm and results were compared to the static control.

Statistical analysis

The data were analyzed using GraphPad Prism version 5 (GraphPad Software, San Diego, CA). Quantitative data were analyzed using the Dunn's nonparametric comparison for post-hoc testing after the Kruskal-Wallis test. $P < 0.05$ was considered significant.

Results

Gene expressions in HTM cells in response to shear tress

Our microarray analysis investigated 62,976 genes. Among those, we focused on representative genes related to ECM metabolism and compared the gene expression levels of the static control to those exposed to shear stress (0.2 dyne/cm^2) for 12 hours. The gene

categories, names, and fold changes are shown in Table 2. Those genes listed then were analyzed by real-time RT-PCR to ascertain the results obtained by microarray analysis. As a result, transforming growth factor (TGF)-β2 mRNA levels were significantly lower than that of the static control (0.2 dyne/cm^2, 0.65-fold vs. static control, $p < 0.01$) (Fig. 1). The MMP2 mRNA levels were significantly higher (0.2 dyne/cm^2, 2.35-fold vs. static control, $p < 0.05$ and 1.0 dyne/cm^2, 2.96-fold vs. static control, $p < 0.05$) (Fig. 2A), while the differences in the TIMP2 mRNA levels were not significant (0.2 dyne/cm^2, 1.49-fold vs. static control, and 1.0 dyne/cm^2, 2.03-fold vs. static control, $p = 0.055$) (Fig. 2B) The COL type 1 alpha 2 (COL1A2) mRNA (1.0 dyne/cm^2, 1.79-fold vs. static control, $p < 0.05$), COL type 4 alpha 2 (COL4A2) mRNA (1.0 dyne/cm^2, 3.11-fold vs. static control, $p< 0.01$), and COL type 6 alpha 1 (COL6A1) mRNA (1.0 dyne/cm^2, 1.91-fold vs. static control, $p<0.05$) levels were significantly higher than the static control. Although the FN1 mRNA levels were higher than the static control (1.0 dyne/cm^2, 1.87-fold vs. static control), the differences were not significant ($p = 0.085$) (Fig. 3).

Table 2. Comparison of Gene Expression Levels of the Static Control with Those Exposed to Shear Stress (0.2 dyne/cm^2) for 12 Hours.

Gene Category	Gene Name (symbol)	Accession Number	Fold Change (vs. static control)
TGF-β family	TGF-β1	NM_000660	1.71
	TGF-β2	NM_003238	0.52
	TGF beta receptor 2 (TGFβR2)	NM_001024847	0.60
	Bone morphogenetic protein 5 (BMP5)	NM_021073	0.29
	BMP6	NM_001718	3.49
ECM	COL1A2	NM_000089	0.92
	COL2A1	NM_001844	1.05
	COL3A1	NM_000090	0.62
	COL4A2	NM_001846	1.47
	COL5A2	NM_000093	0.74
	COL6A1	NM_001848	1.00
	FN1	NM_054034	1.41
	Elastin	NM_001278939	2.07
	Laminin β3	NM_001017402	2.27
ECM remodeling	MMP1	NM_002421	3.01
	MMP2	NM_004530	2.24
	MMP3	NM_002422	3.26
	MMP9	NM_004994	1.23
	TIMP1	NM_003254	1.04
	TIMP2	NM_003255	0.99
	Plasminogen activator inhibitor type 1	NM_000602	11.91
	Connective tissue growth factor	NM_001901	1.99

Fig. 1. Real-time RT-PCR analysis of TGF-β2 mRNA expression in HTM cells. TGF-β2 mRNA levels in the HTM cells exposed to shear stress (0.2 dyne/cm^2) for 12 hours are significantly lower than the static control. The data are expressed as the means ± standard deviation (n = 5). *p < 0.01.

Fig. 2. Real-time RT-PCR analysis of MMP2 mRNA and TIMP2 mRNA expression in HTM cells. (A) MMP2 mRNA levels in the HTM cells exposed to shear stress (0.2 and 1 dyne/cm^2) for 12 hours are significantly higher than the static control. (B) Although TIMP2 mRNA levels are higher than the static control after stimulation, the differences are not significant. The data are expressed as the means ± standard deviation (n = 5). *p < 0.05.

Fig. 3. Real-time RT-PCR analysis of COL1A2, COL4A2, COL6A1, and FN1 mRNA expression in HTM cells. COL1A2, COL4A2, and COL6A1 mRNA levels in the HTM cells exposed to shear stress (1 dyne /cm^2) for 12 hours are significantly higher than the static control. Although the FN1 mRNA levels are higher than the static control after stimulation, the differences are not significant. The data are expressed as the means ± standard deviation (n = 4). *p < 0.05 and **p < 0.01.

232

233 **FN and COL IV levels in the supernatant after exposure to shear stress**

234 The mean (± standard deviation) FN levels (ng/mL) in the medium exposed to shear stress
235 (dyne/cm^2) of 0, 0.2, and 1.0 for 1 hour were 31.6 ± 19.6, 30.0 ± 18.7, and 29.5 ± 13.6,
236 respectively. The values for 12 hours were 193.7 ± 7.6, 51.5 ± 21.8, and 34.9 ± 23.6,
237 respectively. After 12 hours, the FN levels were significantly ($p < 0.01$) lower at 1.0
238 dyne/cm^2 than the static control (Fig. 4). Representative images of each band obtained by
239 Western blot analysis are shown in Fig. 5A. The FN levels were significantly lower at 0.2
240 dyne/cm^2 ($p < 0.05$) and 1.0 dyne/cm^2 ($p < 0.01$) than the static control. The COL IV
241 levels at 1.0 dyne/cm^2 also were significantly ($p < 0.01$) lower than the static control (Fig.
242 5B).

243

244 **Fig. 4. The concentration of FN in the culture supernatant after exposure to shear**
245 **stress.** After exposure to shear stress (1 dyne /cm^2) for 12 hours, the levels of FN are
246 significantly lower than the static control. The data are expressed as the means ± standard
247 deviation ($n = 5$). **$p < 0.01$. hr, hours.

248

249 **Fig. 5. FN and COL IV levels in HTM cells after exposure to shear stress.** (A)

Representative images of Western blot analysis of FN and COL IV expression. (B) Quantitative assessment of the intensity of each band determined by densitometry. The FN and COL IV levels are significantly lower compared to the static control after stimulation. The data are expressed as the means ± standard deviation (FN, n = 6; COL IV, n = 5). *p < 0.05 and **p < 0.01.

ROCK activity in HTM cells after exposure to shear stress

To examine the ROCK activity, we carried out the ELISA technique. Our experiment showed that the ROCK activity was significantly lower than the static control after exposure to shear stress (0.2 dyne/cm^2, 0.78-fold vs. static control, $p < 0.05$) (Fig. 6).

Fig. 6. **ROCK activity in HTM cells after exposure to shear stress.** The ROCK activity is significantly lower than the static control after exposure to shear stress (0.2 dynes/cm^2) for 12 hours. The data are expressed as means ± standard deviation (n = 4). *p < 0.05.

Discussion

In the current study, we applied shear stress to HTM cells and investigated the changes in gene or protein expressions related to ECM metabolism. Because FN, laminin, and COL

IV are the main ECM components of the JCT [6], we focused on those components in our experiments. As a result, FN and COL IV levels in the supernatant, in which HTM cells were exposed to shear stress for sufficient time, were significantly lower than the static control. This implies that FN and COL IV production by HTM cells are suppressed in the presence of shear stress. Our microarray analysis and subsequent real-time RT-PCR also showed lower levels of TGF-β2 mRNA and elevated levels of MMP2 mRNA expression with increased shear stress. Because down-regulation of TGF-β2 and the increased MMP2 promote ECM degradation, HTM cells may promote degradation of the ECM in the presence of shear stress. Regarding the increases in COL mRNA and FN1 mRNA, we considered these as compensatory responses (i.e., negative feedback mechanism). Our results agreed with previous reports that examined the effects of mechanical stimulation by stretching [21, 22] or IOP pulsation on TM cells in that the mechanical stimulation might have an important role in ECM turnover in the TM [12].

Previously, fluid flow stress was reported to affect the pathological condition or homeostasis in some ocular tissues, e.g., flow stress on cultured human corneal epithelial cells affected TGF-β signaling, which may be associated with a delayed wound-healing mechanism during blinking [20]. Flow stress also can cause corneal endothelial cell damage or loss after laser iridotomy [23] or gene expression of endovascular cells, which

may contribute to the vasoregulatory and antithrombotic properties of the retinal vessels [18]. Although the current study focused on mechanical stimulation of the fluid flow on the HTM cells, a previous report also investigated the responses of HTM cells exposed to shear stress. Ashpole et al. [24] reported that when shear stress (10 dyne/cm^2) was applied to human SC endothelial (SCE) cells, they responded similarly to vascular endothelial cells, i.e., shear stress also triggered nitric oxide (NO) production on human SCE cells. Those authors concluded that increased shear stress to SCE cells during SC collapse in the presence of elevated IOP may partly mediate IOP homeostasis by NO production. Although, in that study, they also investigated the responses of HTM cells exposed to a shear stress (10 dyne/cm^2), they only focused on NO production. In the current study, we applied shear stress to HTM cells, but the strength was very weak (0.2 or 1.0 dyne/cm^2). Therefore, the current study differed from their research in that we focused on the gene or protein changes related to ECM metabolism in response to very weak shear stress.

In our microarray analysis, we focused on the gene changes related to the TGF-β superfamily and ECM components and remodeling. As a result, the expression of TGF-β1 mRNA was observed, although it could not be confirmed by subsequent real-time RT-PCR in our experiments. A previous study reported increased production of TGF-β1 after cyclic mechanical stress in the TM [9]. Further, the increased expression of connective

tissue growth factor (CTGF) mRNA and plasminogen activator inhibitor-1 mRNA also were observed, suggesting changes in many genes involved in ECM metabolism when share stress was applied to HTM cells. The simultaneous increase of TGF-β1 mRNA and CTGF mRNA may be reasonable, because CTGF is also up-regulated by TGF-β1 [25]. Regarding bone morphogenetic protein (BMP) 5, which was down-regulated in the current study, it is expressed in the TM and is involved in the normal formation and function of the TM [26]. Although the role of BMP6 in the TM has not been yet elucidated, altered expression of members of the BMP family may cause functional changes in the TM [27].

In the current study, the ROCK activity in the HTM cells after stimulation was lower than the static control. Because the fibrogenic effect caused by TGF-β2 is mediated by activating ROCK, the decreased ROCK activity may contribute partly to decreased production of FN and COL IV. The recently launched anti-glaucoma drug ROCK inhibitor (ripasudil) acts on the conventional outflow pathway and decreases IOP by increasing aqueous humor outflow through diverse mechanisms [28, 29]. Among the actions of ripasudil on the TM-SC pathway, the inhibition of ECM production [30] and the suppression of TM cell contraction were considered as the functions targeting the JCT [31]. Given the current results, improvement of the aqueous humor outflow through the TM by ripasudil may further promote the ECM metabolism, contributing to further

322 decreases in IOP when the drug is used over the long term.

323 Although, in the current study, the HTM cells were stimulated by steady fluid flow
324 using our shear stress experimental system, it is presumed that the fluid flow in the TM is
325 probably not a laminar or steady flow in normal eyes. A previous report that simulated the
326 wall shear stress in each component of the conventional outflow pathway reported that the
327 shear stress on the inner wall of the SC was about 0.01 dyne/cm^2 [32]. Therefore, in the
328 JCT, which is the principal tissue of the ECM metabolism in the TM, the shear stress
329 might be equal to or less than that in the inner wall of the SC (i.e., much weaker
330 stimulation than the current experiment). Further, it also has been reported that the TM
331 tissue pulsates in conjunction with the heart rate [33, 34]. Taken together, considering this
332 histologic feature of the meshwork, the aqueous outflow in the TM may be turbulent.
333 Further investigation is needed to determine if the results of the current shear stress
334 experiment also occur in vivo.

335 In conclusion, gene and protein changes related to ECM metabolism were observed
336 as a result of culturing of the HTM cells in the presence of shear stress. The current results
337 suggested that the mechanical stimulation of aqueous fluid flow to the TM promotes ECM
338 turnover, contributing to maintenance of IOP homeostasis in normal eyes.

339

340

341 # Acknowledgments

342 We are grateful to C. Matsumoto and A. Tanner for their excellent technical assistance.

343

344 # Author contributions

345 Conceived and designed the experiments: KY, MK, TU, YT, AI. Performed the

346 experiments: KY. Analyzed the data: KY, MK, YS, MU. Contributed

347 reagents/materials/analysis tools: MK, TU, AI, AY. Wrote the paper: KY, MK.

348

References

1. Brubaker RF. The measurement of pseudofacility and true facility by constant pressure perfusion in the normal rhesus monkey eye. Investigative ophthalmology. 1970;9(1):42-52. Epub 1970/01/01. PubMed PMID: 4983461.

2. Tamm ER. The trabecular meshwork outflow pathways: structural and functional aspects. Exp Eye Res. 2009;88(4):648-55. Epub 2009/02/26. doi: 10.1016/j.exer.2009.02.007. PubMed PMID: 19239914.

3. Acott TS, Kelley MJ, Keller KE, Vranka JA, Abu-Hassan DW, Li X, et al. Intraocular pressure homeostasis: maintaining balance in a high-pressure environment. J Ocul Pharmacol Ther. 2014;30(2-3):94-101. Epub 2014/01/10. doi: 10.1089/jop.2013.0185. PubMed PMID: 24401029; PubMed Central PMCID: PMCPMC3991985.

4. Brubaker RF. Flow of aqueous humor in humans [The Friedenwald Lecture]. Invest Ophthalmol Vis Sci. 1991;32(13):3145-66. Epub 1991/12/01. PubMed PMID: 1748546.

5. Johnson M. 'What controls aqueous humour outflow resistance?'. Exp Eye Res. 2006;82(4):545-57. Epub 2006/01/03. doi: 10.1016/j.exer.2005.10.011. PubMed PMID: 16386733; PubMed Central PMCID: PMCPMC2892751.

6. Ueda J, Wentz-Hunter K, Yue BY. Distribution of myocilin and extracellular matrix components in the juxtacanalicular tissue of human eyes. Invest Ophthalmol Vis Sci. 2002;43(4):1068-76. Epub 2002/03/30. PubMed PMID: 11923248.

7. Vranka JA, Kelley MJ, Acott TS, Keller KE. Extracellular matrix in the trabecular meshwork: intraocular pressure regulation and dysregulation in glaucoma. Exp Eye Res. 2015;133:112-25. Epub 2015/03/31. doi: 10.1016/j.exer.2014.07.014. PubMed PMID: 25819459; PubMed Central PMCID: PMCPMC4379427.

8. Bradley JM, Kelley MJ, Rose A, Acott TS. Signaling pathways used in trabecular matrix metalloproteinase response to mechanical stretch. Invest Ophthalmol Vis Sci. 2003;44(12):5174-81. Epub 2003/11/26. PubMed PMID: 14638714.

9. Liton PB, Liu X, Challa P, Epstein DL, Gonzalez P. Induction of TGF-beta1 in the trabecular meshwork under cyclic mechanical stress. J Cell Physiol. 2005;205(3):364-71. Epub 2005/05/17. doi: 10.1002/jcp.20404. PubMed PMID: 15895394; PubMed Central PMCID: PMCPMC3143836.

10. Vittal V, Rose A, Gregory KE, Kelley MJ, Acott TS. Changes in gene expression by trabecular meshwork cells in response to mechanical stretching. Invest Ophthalmol Vis Sci. 2005;46(8):2857-68. Epub 2005/07/27. doi: 10.1167/iovs.05-0075. PubMed PMID: 16043860.

385 11. Bradley JM, Kelley MJ, Zhu X, Anderssohn AM, Alexander JP, Acott TS.
386 Effects of mechanical stretching on trabecular matrix metalloproteinases. Invest
387 Ophthalmol Vis Sci. 2001;42(7):1505-13. Epub 2001/05/31. PubMed PMID: 11381054.
388 12. Ramos RF, Stamer WD. Effects of cyclic intraocular pressure on conventional
389 outflow facility. Invest Ophthalmol Vis Sci. 2008;49(1):275-81. Epub 2008/01/04. doi:
390 10.1167/iovs.07-0863. PubMed PMID: 18172103; PubMed Central PMCID:
391 PMCPMC2365474.
392 13. Ramos RF, Sumida GM, Stamer WD. Cyclic mechanical stress and trabecular
393 meshwork cell contractility. Invest Ophthalmol Vis Sci. 2009;50(8):3826-32. Epub
394 2009/04/03. doi: 10.1167/iovs.08-2694. PubMed PMID: 19339745; PubMed Central
395 PMCID: PMCPMC2753281.
396 14. Acott TS, Kelley MJ. Extracellular matrix in the trabecular meshwork. Exp Eye
397 Res. 2008;86(4):543-61. Epub 2008/03/04. doi: 10.1016/j.exer.2008.01.013. PubMed
398 PMID: 18313051; PubMed Central PMCID: PMCPMC2376254.
399 15. Keller KE, Aga M, Bradley JM, Kelley MJ, Acott TS. Extracellular matrix
400 turnover and outflow resistance. Exp Eye Res. 2009;88(4):676-82. Epub 2008/12/18. doi:
401 10.1016/j.exer.2008.11.023. PubMed PMID: 19087875; PubMed Central PMCID:
402 PMCPMC2700052.

16. Rouhiainen HJ, Terasvirta ME, Tuovinen EJ. Peripheral anterior synechiae formation after trabeculoplasty. Archives of ophthalmology (Chicago, Ill : 1960). 1988;106(2):189-91. Epub 1988/02/01. doi: 10.1001/archopht.1988.01060130199025. PubMed PMID: 3341973.

17. Pattabiraman PP, Rao PV. Mechanistic basis of Rho GTPase-induced extracellular matrix synthesis in trabecular meshwork cells. Am J Physiol Cell Physiol. 2010;298(3):C749-63. Epub 2009/11/27. doi: 10.1152/ajpcell.00317.2009. PubMed PMID: 19940066; PubMed Central PMCID: PMCPMC2838580.

18. Ishibazawa A, Nagaoka T, Takahashi T, Yamamoto K, Kamiya A, Ando J, et al. Effects of shear stress on the gene expressions of endothelial nitric oxide synthase, endothelin-1, and thrombomodulin in human retinal microvascular endothelial cells. Invest Ophthalmol Vis Sci. 2011;52(11):8496-504. Epub 2011/09/08. doi: 10.1167/iovs.11-7686. PubMed PMID: 21896842.

19. Ishibazawa A, Nagaoka T, Yokota H, Ono S, Yoshida A. Low shear stress up-regulation of proinflammatory gene expression in human retinal microvascular endothelial cells. Exp Eye Res. 2013;116:308-11. Epub 2013/10/17. doi: 10.1016/j.exer.2013.10.001. PubMed PMID: 24128656.

20. Utsunomiya T, Ishibazawa A, Nagaoka T, Hanada K, Yokota H, Ishii N, et al.

421 Transforming Growth Factor-beta Signaling Cascade Induced by Mechanical Stimulation
422 of Fluid Shear Stress in Cultured Corneal Epithelial Cells. Invest Ophthalmol Vis Sci.
423 2016;57(14):6382-8. Epub 2016/11/30. doi: 10.1167/iovs.16-20638. PubMed PMID:
424 27898984.

425 21. Okada Y, Matsuo T, Ohtsuki H. Bovine trabecular cells produce TIMP-1 and
426 MMP-2 in response to mechanical stretching. Jpn J Ophthalmol. 1998;42(2):90-4. Epub
427 1998/05/20. PubMed PMID: 9587839.

428 22. WuDunn D. The effect of mechanical strain on matrix metalloproteinase
429 production by bovine trabecular meshwork cells. Curr Eye Res. 2001;22(5):394-7. Epub
430 2001/10/16. PubMed PMID: 11600941.

431 23. Yamamoto Y, Uno T, Joko T, Shiraishi A, Ohashi Y. Effect of anterior chamber
432 depth on shear stress exerted on corneal endothelial cells by altered aqueous flow after
433 laser iridotomy. Invest Ophthalmol Vis Sci. 2010;51(4):1956-64. Epub 2009/11/13. doi:
434 10.1167/iovs.09-4280. PubMed PMID: 19907022.

435 24. Ashpole NE, Overby DR, Ethier CR, Stamer WD. Shear stress-triggered nitric
436 oxide release from Schlemm's canal cells. Invest Ophthalmol Vis Sci. 2014;55(12):8067-
437 76. Epub 2014/11/15. doi: 10.1167/iovs.14-14722. PubMed PMID: 25395486; PubMed
438 Central PMCID: PMCPMC4266075.

439 25. Chudgar SM, Deng P, Maddala R, Epstein DL, Rao PV. Regulation of
440 connective tissue growth factor expression in the aqueous humor outflow pathway. Mol
441 Vis. 2006;12:1117-26. Epub 2006/11/10. PubMed PMID: 17093396.
442 26. Wordinger RJ, Agarwal R, Talati M, Fuller J, Lambert W, Clark AF. Expression
443 of bone morphogenetic proteins (BMP), BMP receptors, and BMP associated proteins in
444 human trabecular meshwork and optic nerve head cells and tissues. Mol Vis. 2002;8:241-
445 50. Epub 2002/07/20. PubMed PMID: 12131877.
446 27. Tamm ER, Fuchshofer R. What increases outflow resistance in primary open-
447 angle glaucoma? Surv Ophthalmol. 2007;52 Suppl 2:S101-4. Epub 2007/12/06. doi:
448 10.1016/j.survophthal.2007.08.002. PubMed PMID: 17998032.
449 28. Tanihara H, Inoue T, Yamamoto T, Kuwayama Y, Abe H, Fukushima A, et al.
450 One-year clinical evaluation of 0.4% ripasudil (K-115) in patients with open-angle
451 glaucoma and ocular hypertension. Acta Ophthalmol. 2016;94(1):e26-34. Epub
452 2015/09/05. doi: 10.1111/aos.12829. PubMed PMID: 26338317.
453 29. Honjo M, Tanihara H. Impact of the clinical use of ROCK inhibitor on the
454 pathogenesis and treatment of glaucoma. Jpn J Ophthalmol. 2018;62(2):109-26. Epub
455 2018/02/16. doi: 10.1007/s10384-018-0566-9. PubMed PMID: 29445943.
456 30. Fujimoto T, Inoue T, Kameda T, Kasaoka N, Inoue-Mochita M, Tsuboi N, et al.

457 Involvement of RhoA/Rho-associated kinase signal transduction pathway in
458 dexamethasone-induced alterations in aqueous outflow. Invest Ophthalmol Vis Sci.
459 2012;53(11):7097-108. Epub 2012/09/13. doi: 10.1167/iovs.12-9989. PubMed PMID:
460 22969074.

461 31. Koga T, Koga T, Awai M, Tsutsui J, Yue BY, Tanihara H. Rho-associated
462 protein kinase inhibitor, Y-27632, induces alterations in adhesion, contraction and
463 motility in cultured human trabecular meshwork cells. Exp Eye Res. 2006;82(3):362-70.
464 Epub 2005/08/30. doi: 10.1016/j.exer.2005.07.006. PubMed PMID: 16125171.

465 32. Villamarin A, Roy S, Hasballa R, Vardoulis O, Reymond P, Stergiopulos N. 3D
466 simulation of the aqueous flow in the human eye. Med Eng Phys. 2012;34(10):1462-70.
467 Epub 2012/03/16. doi: 10.1016/j.medengphy.2012.02.007. PubMed PMID: 22417975.

468 33. Li P, Shen TT, Johnstone M, Wang RK. Pulsatile motion of the trabecular
469 meshwork in healthy human subjects quantified by phase-sensitive optical coherence
470 tomography. Biomed Opt Express. 2013;4(10):2051-65. Epub 2013/10/25. doi:
471 10.1364/BOE.4.002051. PubMed PMID: 24156063; PubMed Central PMCID:
472 PMCPMC3799665.

473 34. Johnstone MA. Intraocular pressure regulation: findings of pulse-dependent
474 trabecular meshwork motion lead to unifying concepts of intraocular pressure

475 homeostasis. J Ocul Pharmacol Ther. 2014;30(2-3):88-93. Epub 2013/12/24. doi:
476 10.1089/jop.2013.0224. PubMed PMID: 24359130; PubMed Central PMCID:
477 PMCPMC3991971.

Fig 1

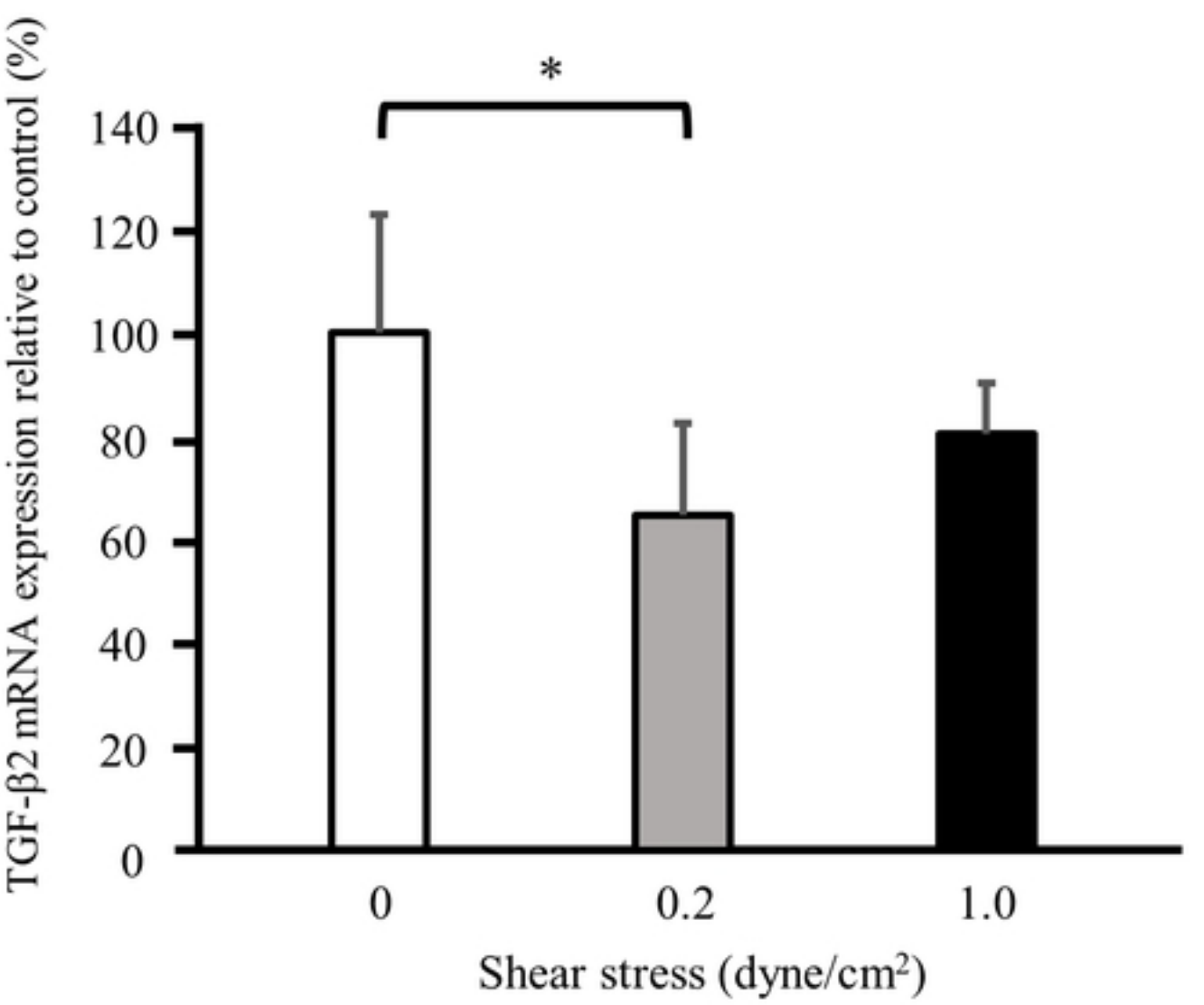

Figure 1

Fig 2

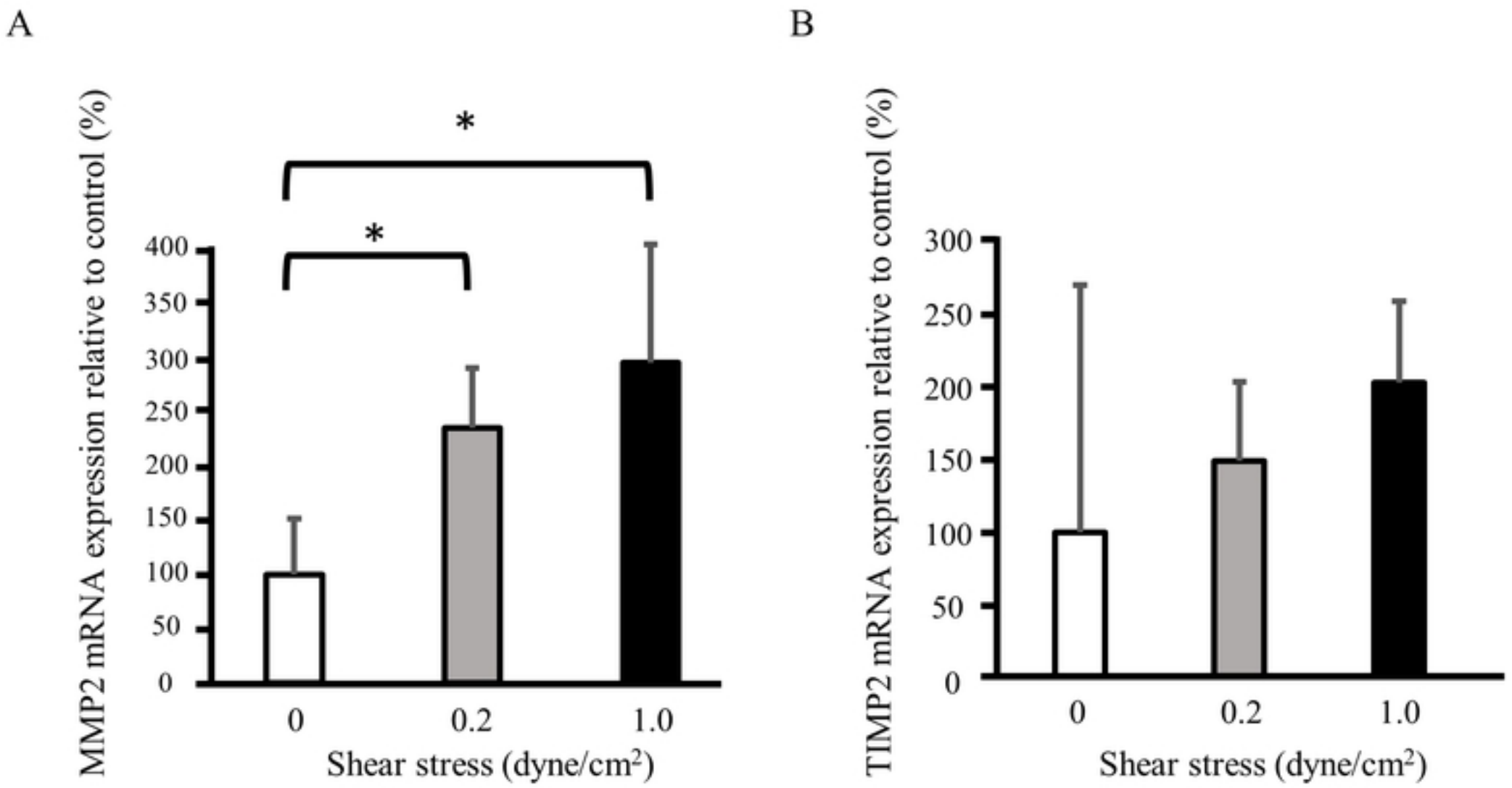

Figure 2

Fig 3

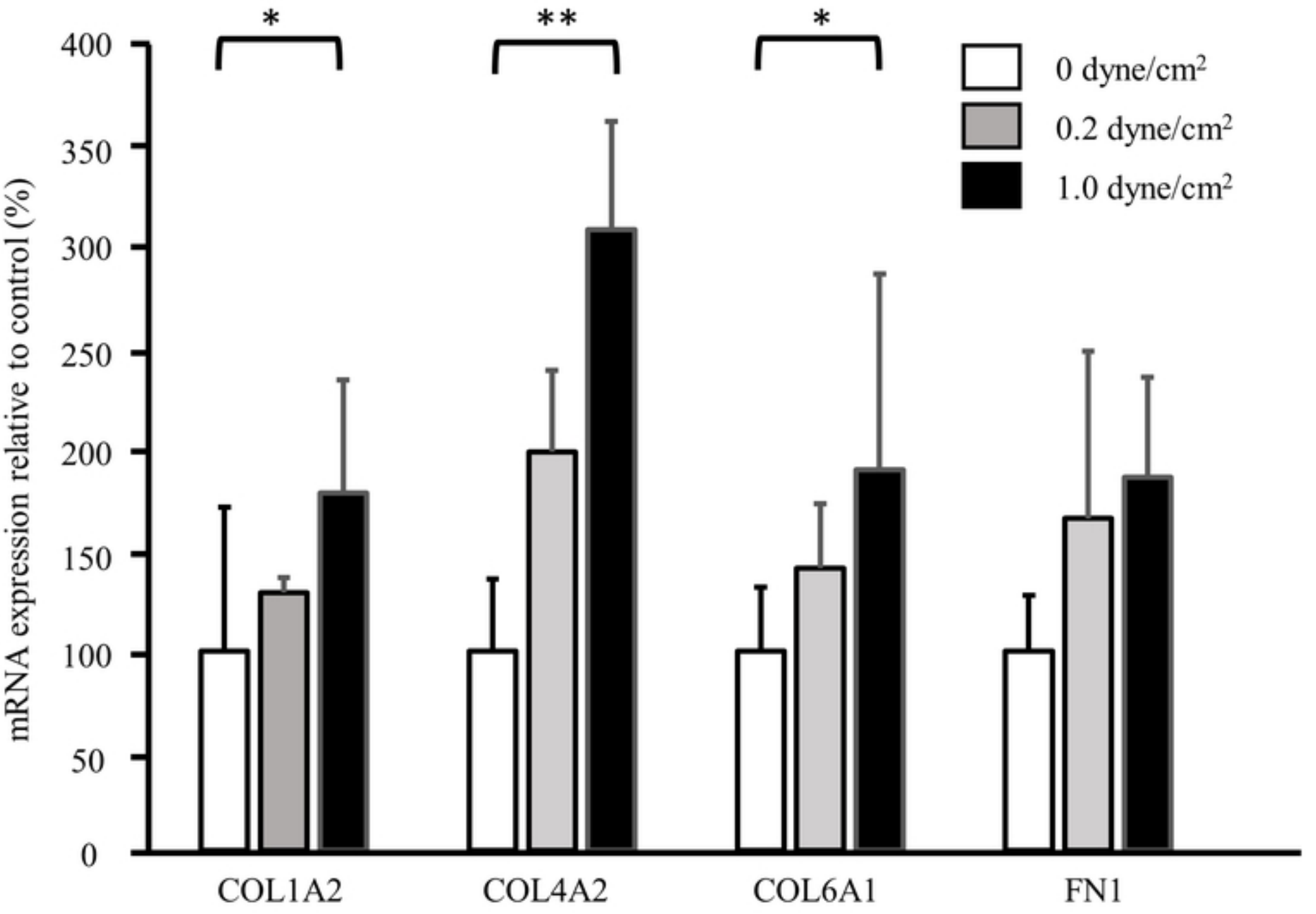

Figure 3

Fig 4

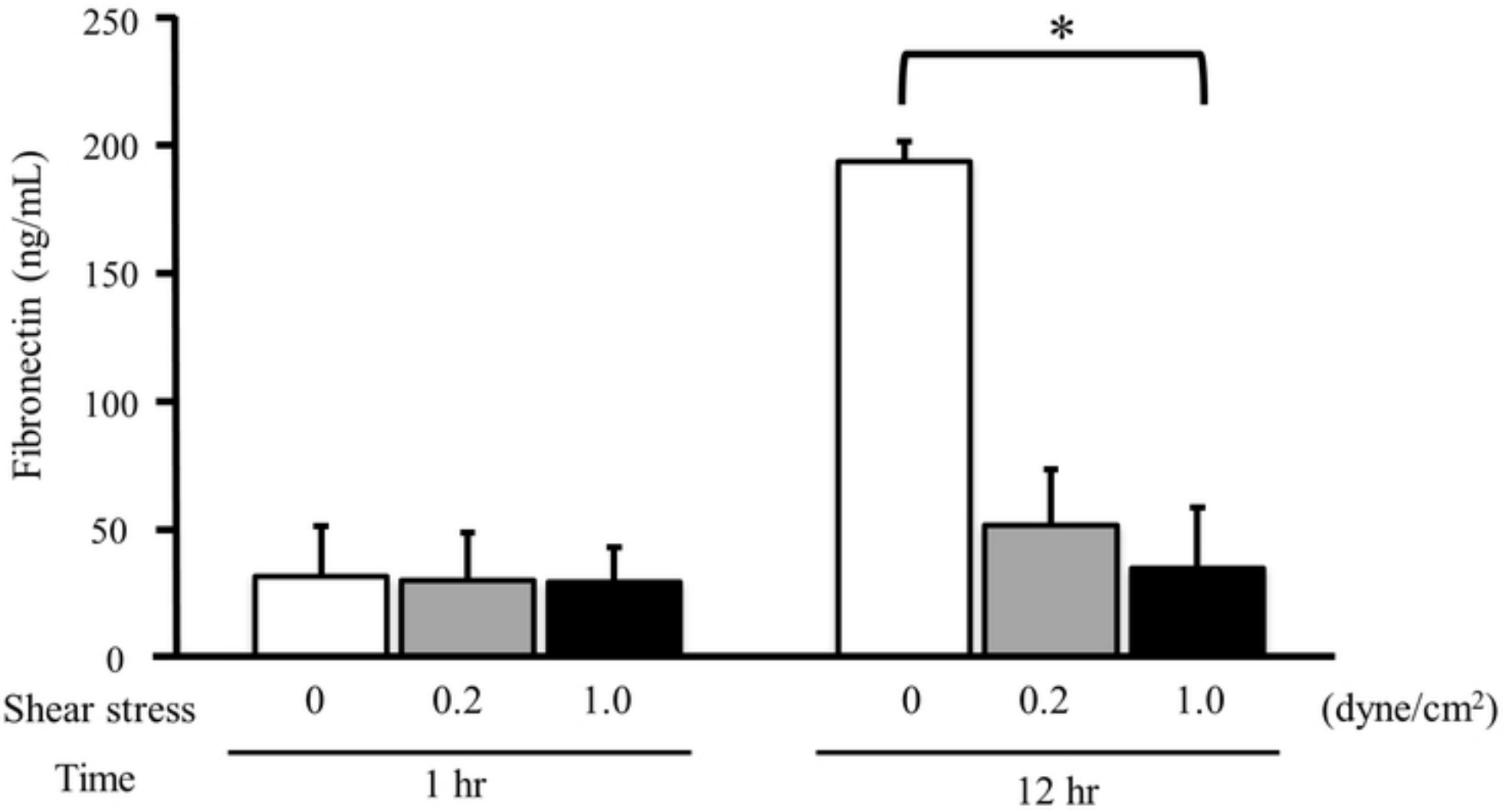

Figure 4

Fig 5

A

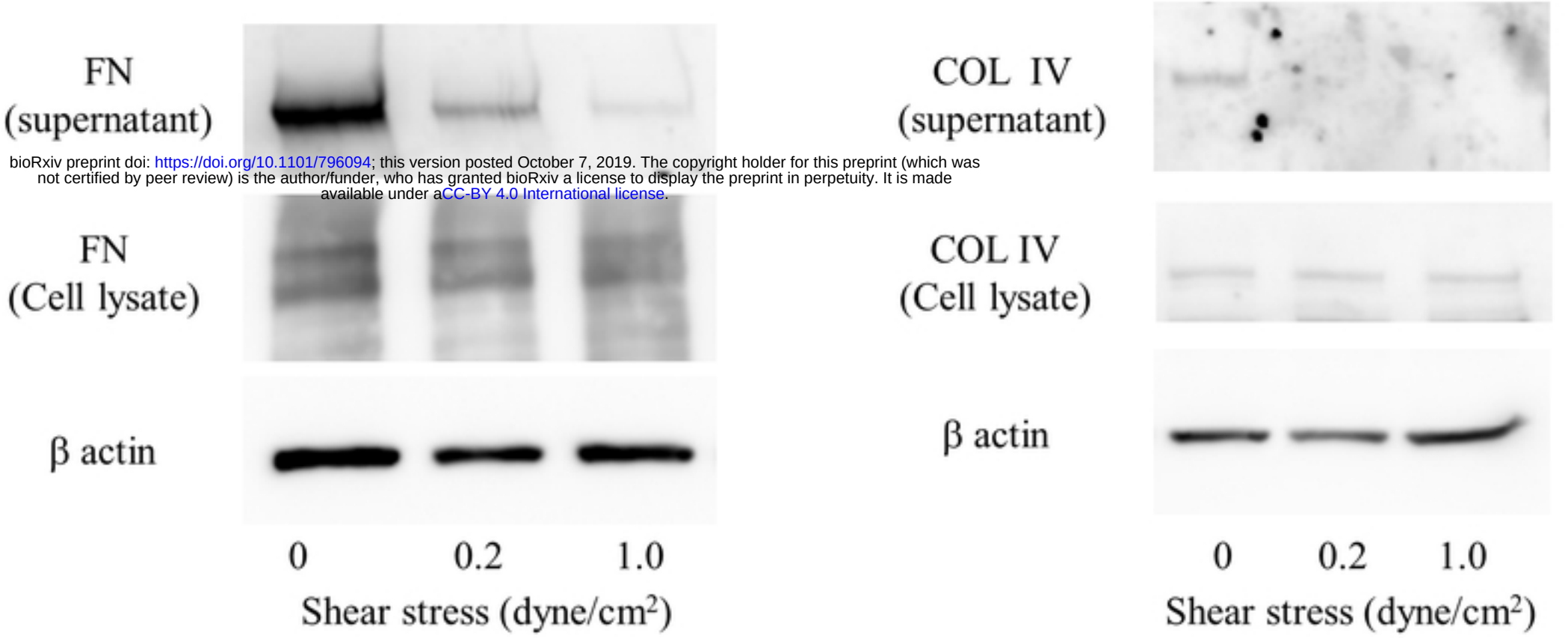

B

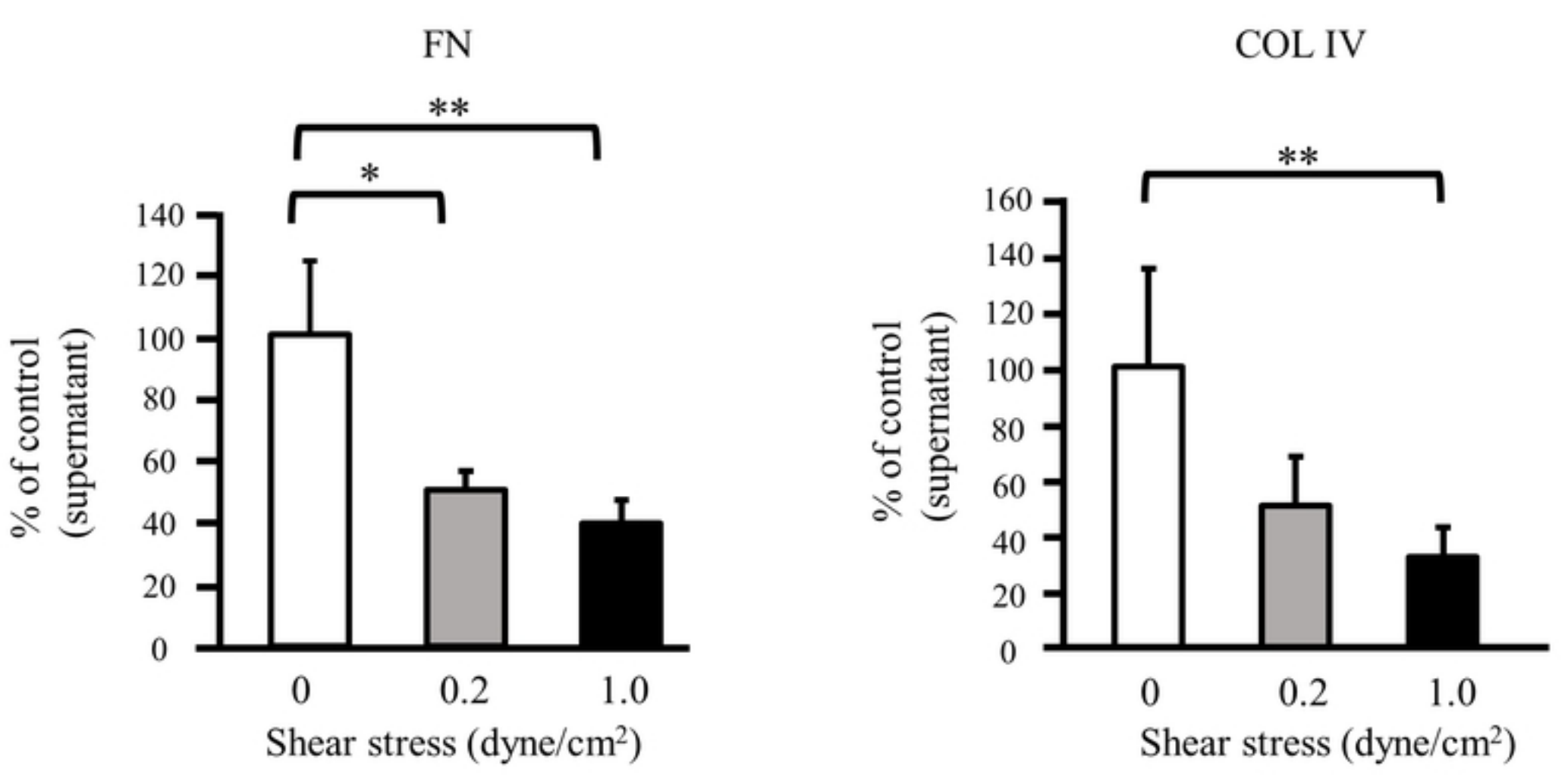

Figure 5

Fig 6

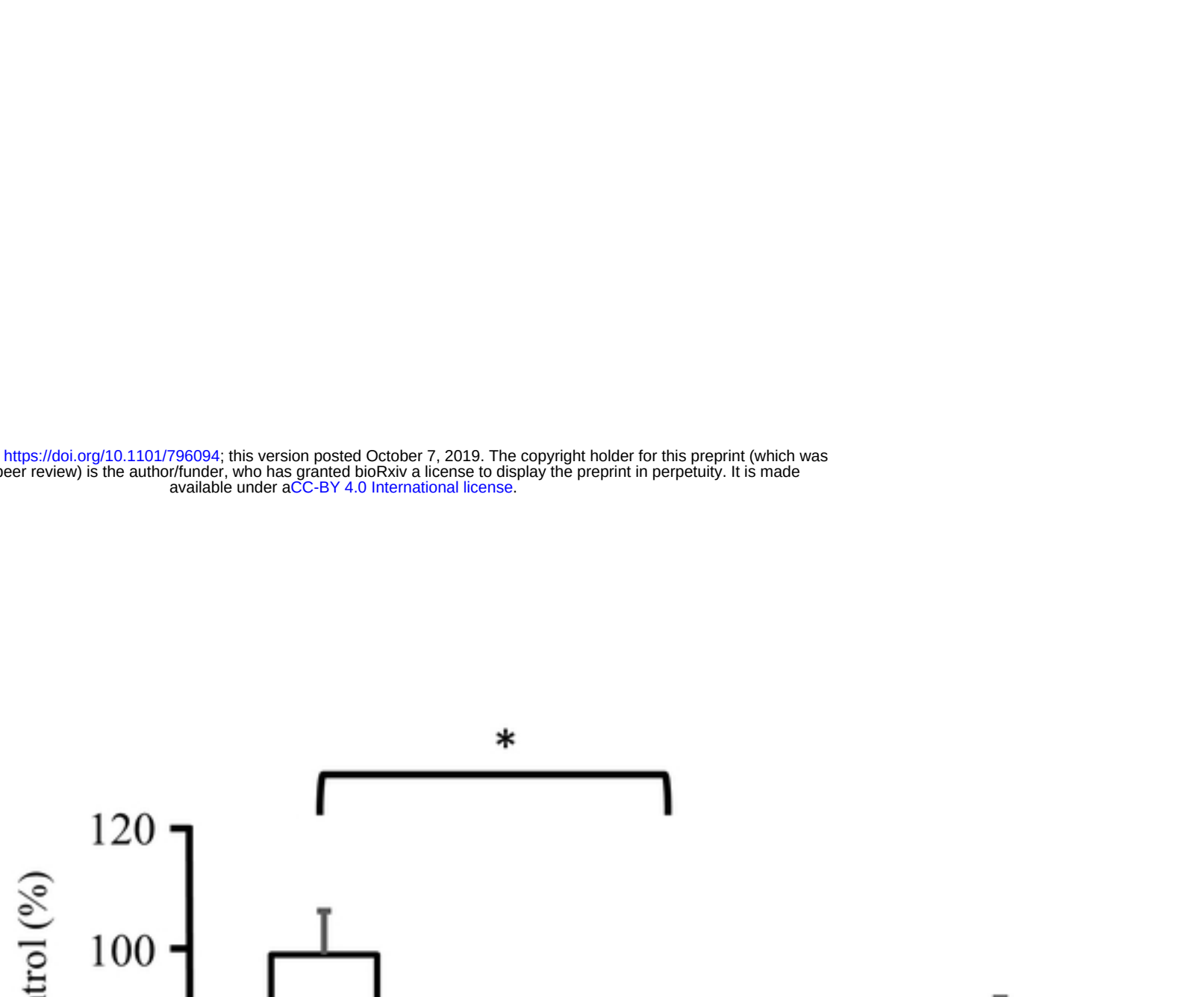

Figure 6